NOTICES

When Government drawings, specifications, or other data are used for any purpose other than in connection with a definitely related Government procurement operation, the United States Government thereby incurs no responsibility nor any obligation whatsoever; and the fact that the Government may have formulated, furnished, or in any way supplied the said drawings, specifications, or other data, is not to be regarded by implication or otherwise as in any manner licensing the holder or any other person or corporation, or conveying any rights or permission to manufacture, use, or sell any patented invention that may in any way be related thereto.

This document is subject to special export controls and each transmittal to foreign governments or foreign nationals may be made only with prior approval of the Metals and Ceramics Division (MAM), Air Force Materials Laboratory, Wright-Patterson Air Force Base, Ohio 45433.

Distribution of this report is limited because the report contains technology identifiable with items on the strategic embargo lists excluded from export under the U. S. Export Control Act, as implemented by ARF 310-2 and AFSC 80-20.

Qualified requesters may obtain copies of this report from the Defense Documentation Center (DDC), Cameron Station, Alexandria, Virginia 22314.

ARPA Order No. 1244

Program Code No. 8D10

Name of Contractor: The Regents of The University of Michigan

Effective Date of Contract: July 1, 1968

Contract Expiration Date: June 30, 1971

Amount of Contract: $125,313.00

Contract No. FF33615-68-C-1703

Principal Investigator: J. R. Frederick
Phone: (313)-764-3387

Short Title of Work: Use of Acoustic Emission in Nondestructive Testing

THE UNIVERSITY OF MICHIGAN

COLLEGE OF ENGINEERING
Department of Mechanical Engineering

Semiannual Report

USE OF ACOUSTIC EMISSION IN NONDESTRUCTIVE TESTING

September 1, 1969 - February 28, 1970

J. R. Frederick

ORA Project 01971

under contract with:

UNITED STATES AIR FORCE
AIR FORCE SYSTEMS COMMAND
AERONAUTICAL SYSTEMS DIVISION
CONTRACT NO. F33615-68-C-1703
WRIGHT PATTERSON AIR FORCE BASE, OHIO

ARPA Order No. 1244
Program Code No. 8D10

administered through:

OFFICE OF RESEARCH ADMINISTRATION ANN ARBOR

June 1970

FOREWORD

This is the third semiannual report on a study of the use of acoustic emission in nondestructive testing. This research is supported by the Advanced Research Project Agency of the Department of Defense and is monitored by the Air Force Materials Laboratory, MANN, under Contract No. F33615-68-C-1703, initiated under ARPA Order 1244, Program Code 8D10. Mr. R. R. Rowand (MANN) is project engineer. This report covers the period from September 1, 1969 to February 28, 1970.

The program is being carried out in the Rheology and Fracture Laboratories of the Mechanical Engineering Department of The University of Michigan. The work is under the direction of Associate Professor J. R. Frederick. Professor David K. Felbeck, Mr. Robert Bill, Mr. Charles Thomas, and Mr. William Bracht have participated in the program.

ABSTRACT

Acoustic emission may be defined as the noise given off spontaneously by solid materials as a result of a sudden relaxation of stresses within the material. Stress relaxation can occur as a result of the nucleation or propagation of cracks, or as a consequence of various elastic or plastic deformation processes. The principal elastic or plastic deformation mechanisms that are sources of acoustic emission in solids are (1) the slip of existing dislocations in a metal, (2) the activation of dislocation sources, (3) twinning, and (4) grain boundary slip. This report describes the results of an investigation into the effects of one microstructure parameter, namely grain size, on acoustic emission. It also describes a method by which acoustic emission phenomena may possibly be used to determine the amount of residual stress in metals.

TABLE OF CONTENTS

LIST OF FIGURES

1.0 INTRODUCTION

One of several possible sources of acoustic emission from metals is dislocation motion. The model being used in the present program to explain the emission process is one proposed by Agarwal, et. al.,[1] namely, that the acoustic emission results from the slip produced by the motion of dislocations which originate from dislocation sources that have been activated by an applied stress. It is assumed in the model that a source continues to operate until it is shut off by the back-stress of piled-up dislocations.

One of the tasks that has been pursued has been to investigate the effect of microstructure on acoustic emission. As a result of this effort it has been found that the amount of acoustic emission produced in 99.99% pure aluminum depends on the grain size of the material in an anomalous way, namely, that a peak value of the emission occurs in this material at a grain size of about 350 microns. Above this grain size the emission decreases and approaches a constant value. Below this peak value, the emission also decreases and approaches zero for grain sizes less than 10 microns at the noise threshold level of 4.0 microvolts used in the tests, the results of which are being reported here.

Another task that is being pursued is the use of acoustic emission to measure residual stresses in metal. The determination of the intensity of residual stresses remaining in a manufactured part after some form of processing has been performed on it is generally carried out by removing successive layers of material and measuring the change in stress in the material adjacent to the removed section. This process makes the part

unusuable. Hence it would be useful to have some method for determining the intensity of residual stresses in a part nondestructively.

Other work in progress involves the acoustic emission from specimens while they are undergoing fatigue or creep, and the development of thermal stressing techniques for inducing emission. The temperatures being used in the latter tests are low enough so that no significant structural changes are produced in the material being tested. The results of these tests will be reported in subsequent progress reports as definitive results are obtained.

2.0 EXPERIMENTAL PROCEDURES

Because of the low level of the acoustic emission phenomena being studied and the range of frequencies (6 to 300 kHz) being used, a low noise-level loading system previously described has been used[2]. Schematic diagrams of the mechanical components and the instrumentation are shown in Figs. 1 and 2.

The load is applied to the specimen by the float and lever system shown in Fig. 1. This is located inside an "audiometric" room to reduce the amount of ambient noise picked up by the detection system. The walls of the room have a transmission loss of 60 dB in the octave band of frequencies of 4800 to 9600 Hz. The room is also electrostatically shielded.

The low noise-level preamplifier is located in the audiometric room adjacent to the test specimen so that the input lead from the PZT-5 transducer can be as short as possible. The specimen is supported by nylon grips to provide further isolation from extraneous noise.

* indicates that acoustic isolation or mismatch material is used.

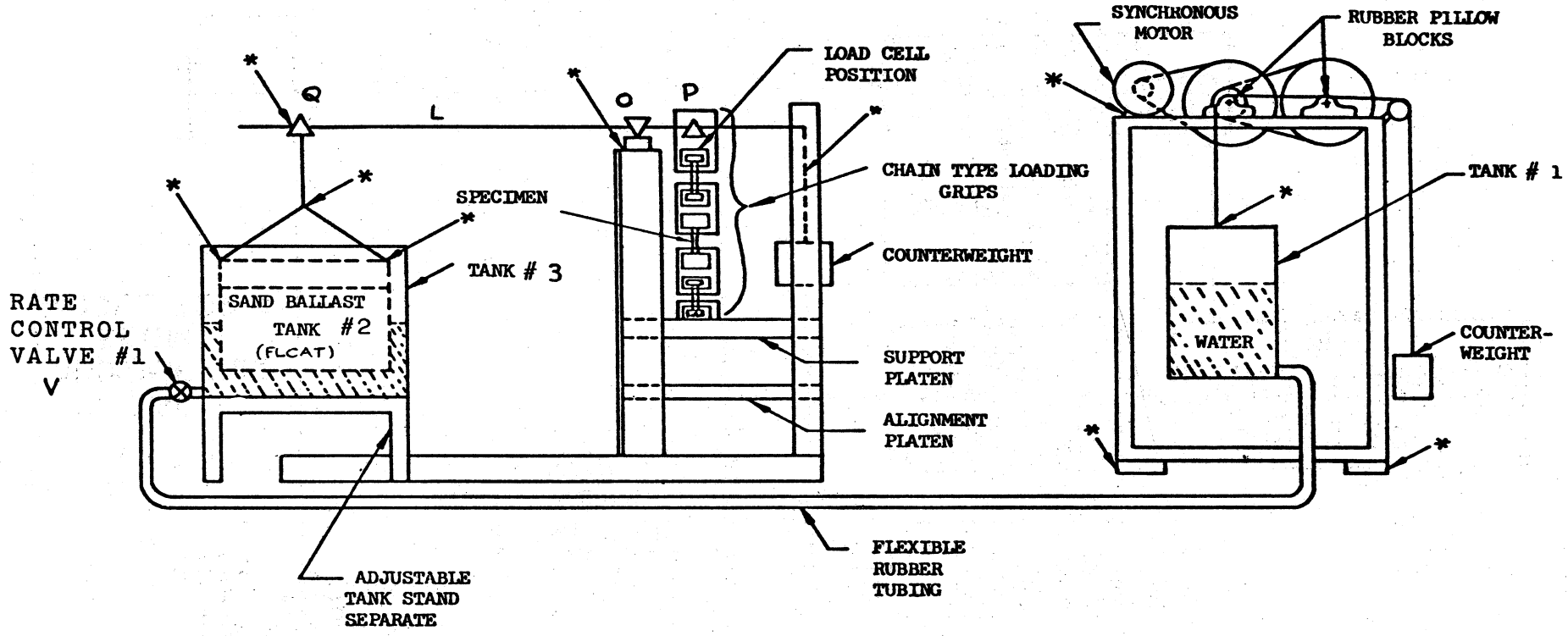

Fig. 1. A float and lever system is used to apply a load to the test specimens. This minimizes the extraneous noise.

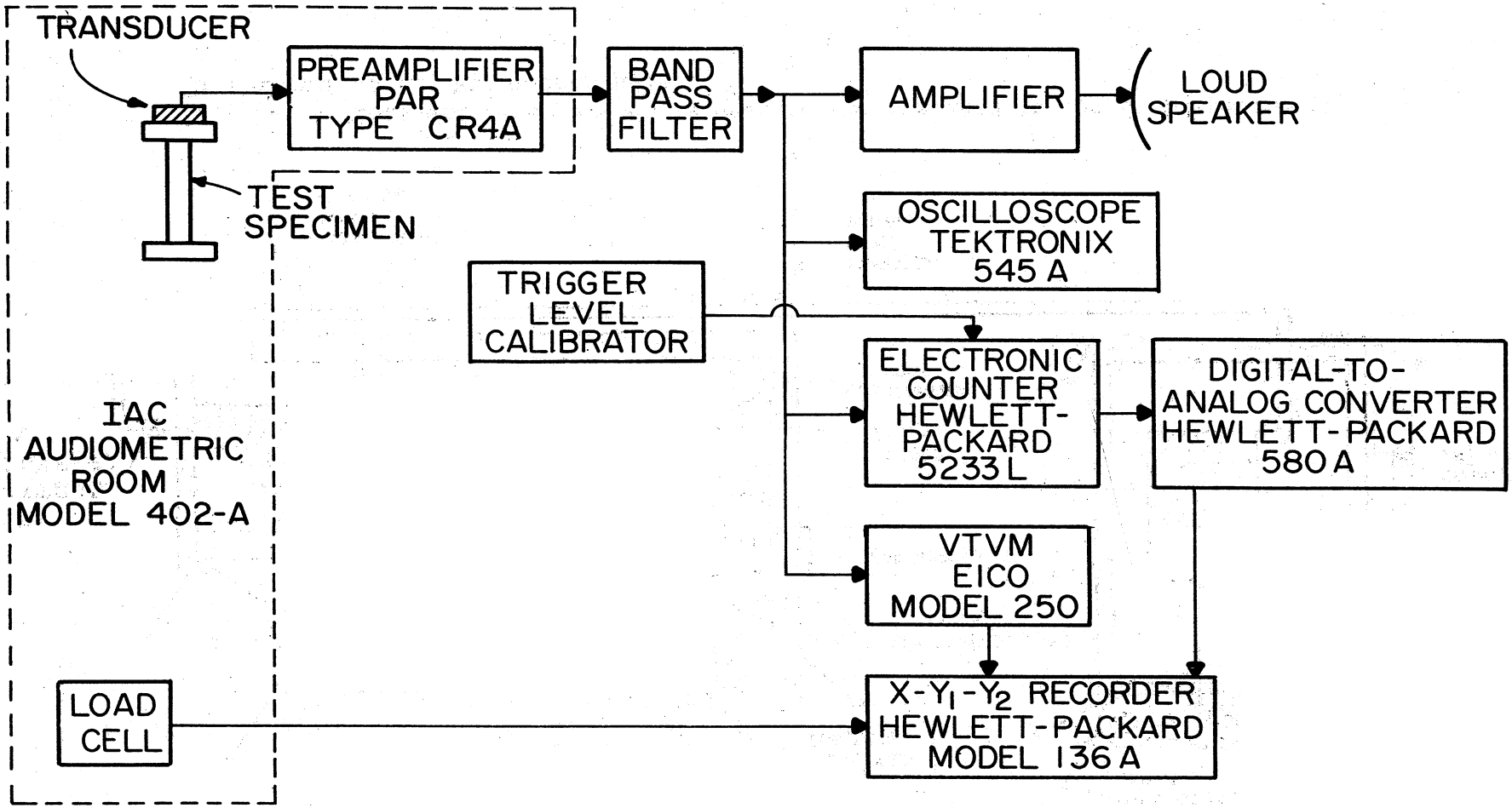

Fig. 2. Block diagram of the electronic components used in the investigation.

3.0 MICROSTRUCTURE INVESTIGATION OF ALUMINUM

The microstructure parameter in 99.99% aluminum that was investigated was grain size. Variations in grain size were obtained by the recrystallization and subsequent grain growth in plastically deformed material.

True-stress, true-strain curves for three different specimens, each of which had a different average grain sizes, are shown in Fig. 3. As is to be expected the smaller the grain size the higher strength.

The cumulative acoustic emission that is obtained for a given applied stress depends on the grain size of the aluminum as shown in Fig. 4. For small or large grain sizes the emission is low, but at an intermediate size there is a maximum total acoustic emission. The bandwidth for the data in Fig. 4 is 80 to 200 kHz. The same shape of curve is also observed in a frequency band of 6 to 20 kHz.

Another effect that is observed concerns the frequency content of the emission. As the grain size increases the amount of emission at low frequencies increases in comparison with the emission at higher frequencies. Fig. 5 shows this effect for three different grain sizes. These data were obtained by analyzing a tape recording of the emission from three different specimens, each of which had a different average grain size. An Ampex FR 100 tape recorder was used to record the acoustic emission. The emission in the various frequency bands was measured by the use of a Krohn-Hite model 310 AB band-pass filter.

3.1 DISCUSSION OF THE RESULTS ON THE EFFECT OF MICROSTRUCTURE ON ACOUSTIC EMISSION

The increase and subsequent decrease in the amount of acoustic emission with increasing grain size can be explained on the basis of the model proposed

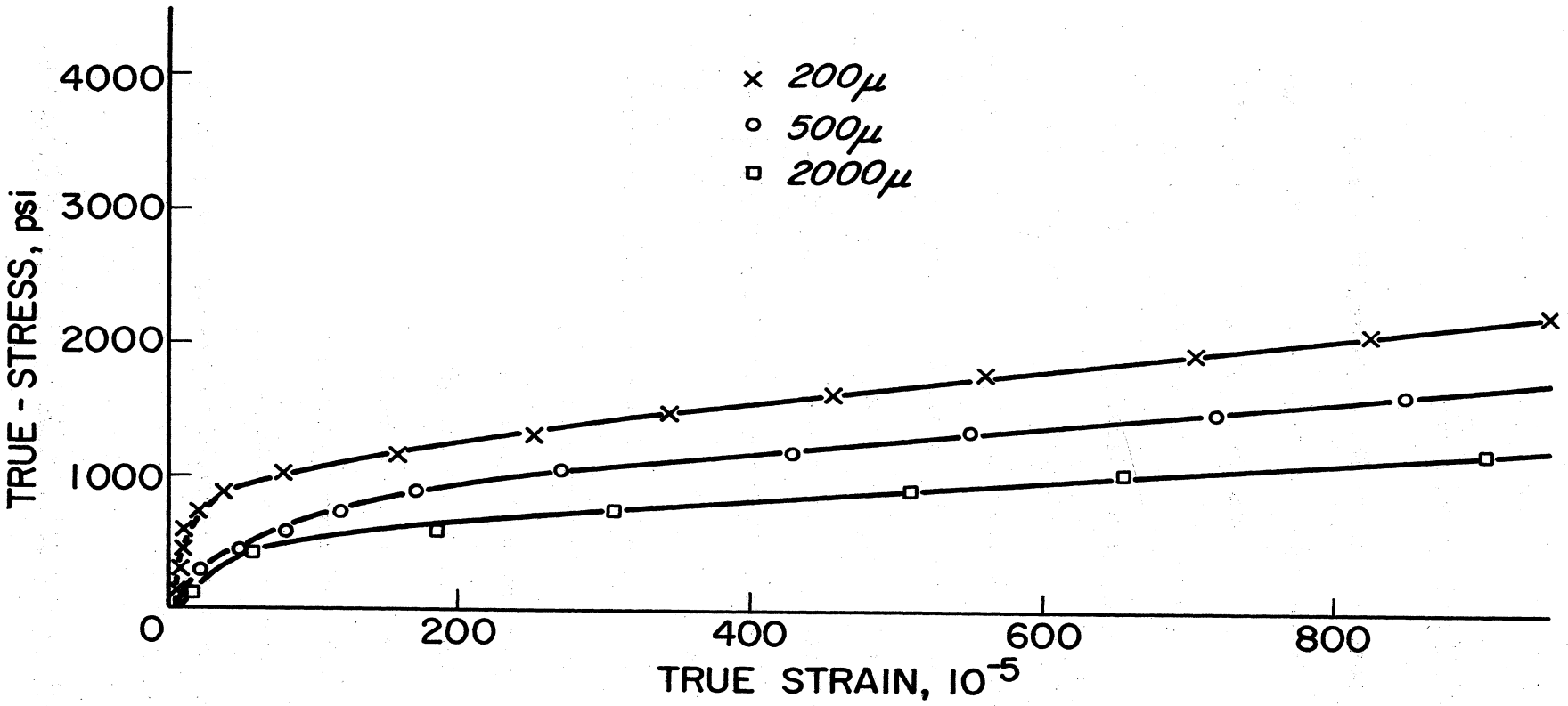

Fig. 3. True-stress, true-strain curves for 99.99% aluminum used in the investigation.

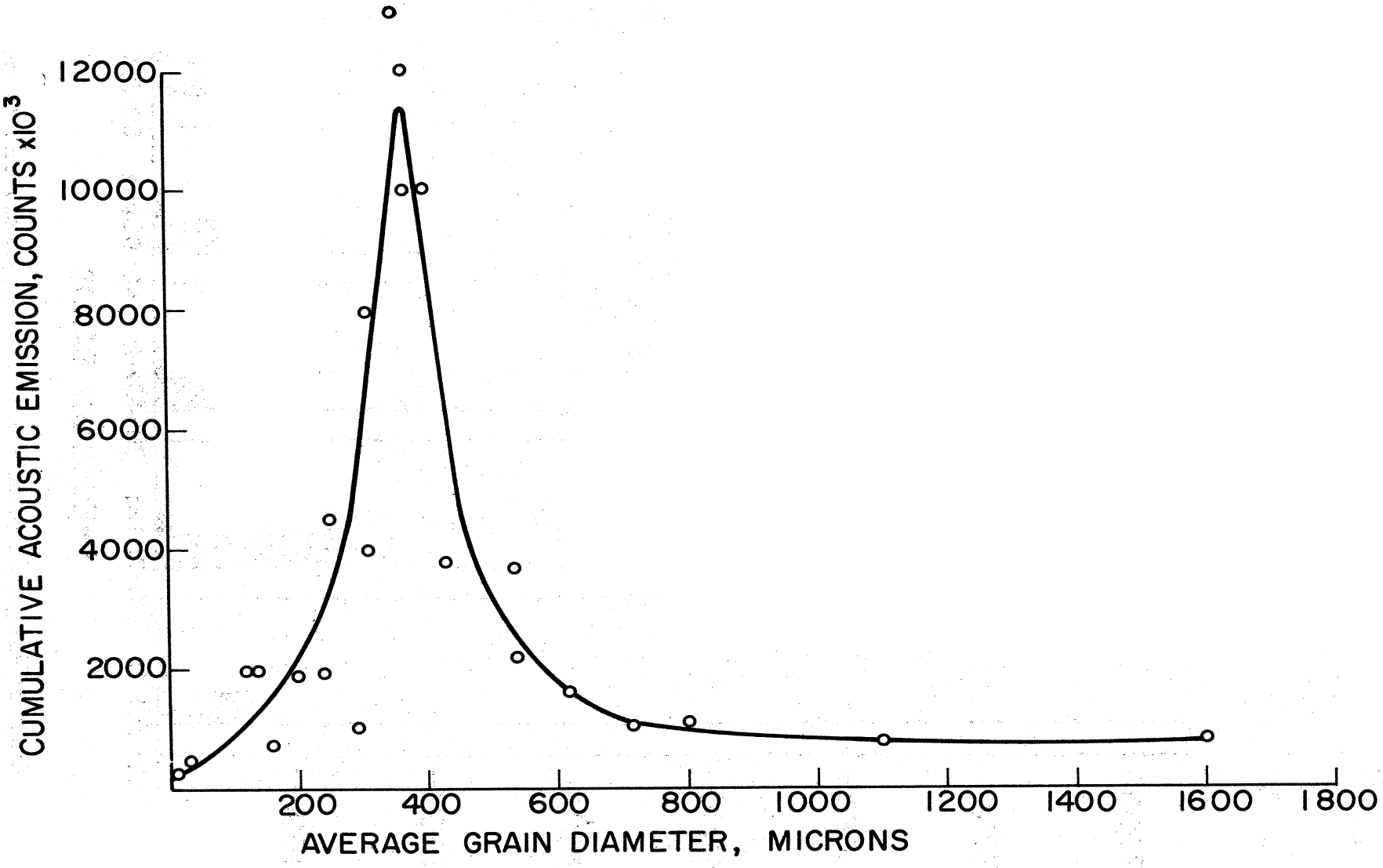

Fig. 4. The cumulative acoustic emission from 99.99% aluminum depends on grain size. The data shown are for a frequency band of 80 to 200 kHz.

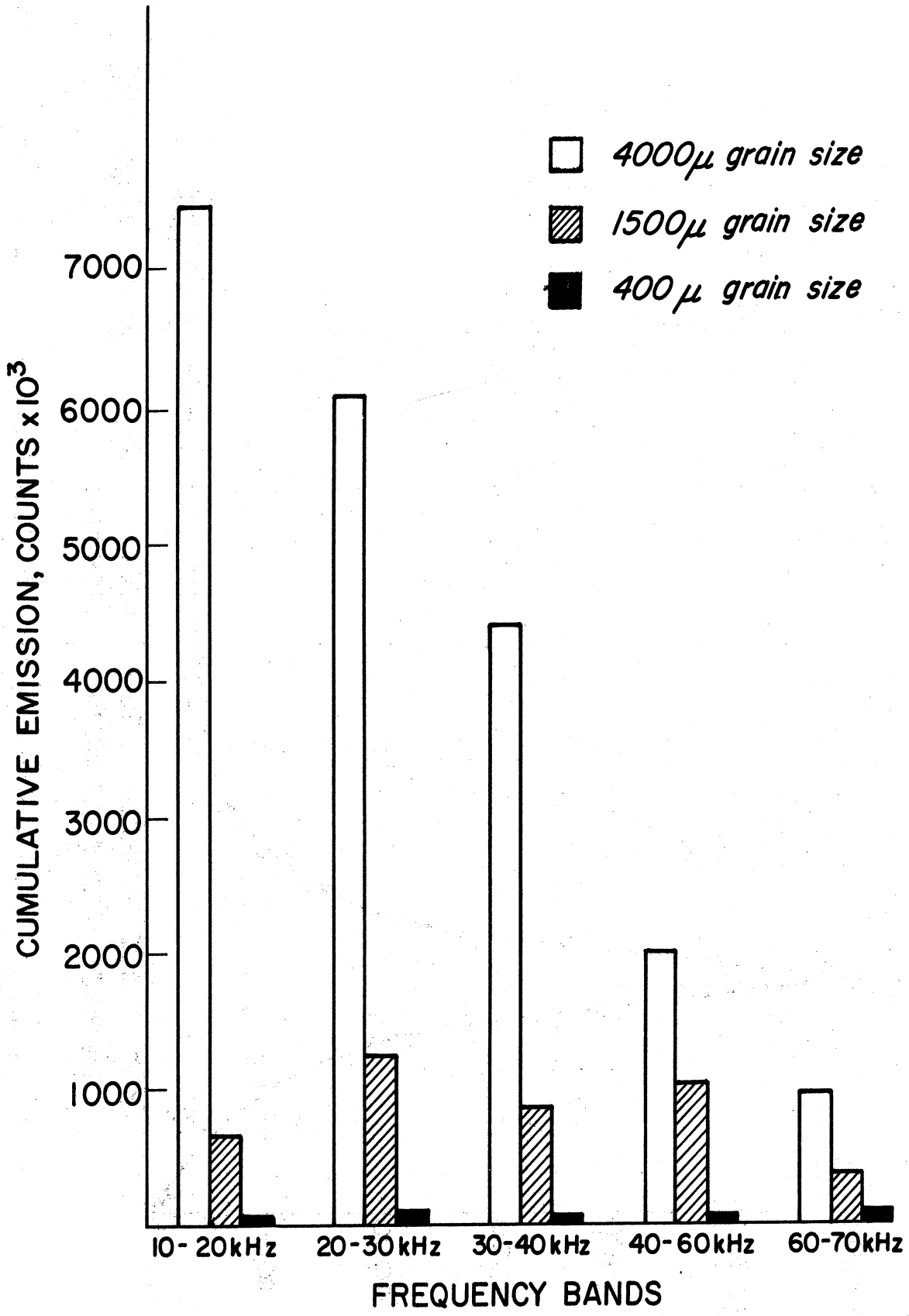

Fig. 5. The acoustic emission from coarse grained 99.99% aluminum is greater at low frequencies than at higher frequencies.

by Agarwal (1). This postulates that acoustic emission is the result of the activation of sources of dislocations by an applied stress. The sources give off avalanches of dislocations until they are shut off because of the back-stress caused by the pile-up of dislocations against obstacles such as a grain boundaries. The generation of an avalanche of dislocations in a short interval of time satisfies the requirement that acoustic emission is only detected if a sufficient amount of slip occurs in a time interval that is short enough so that acoustic signals can be detected by a piezoelectric transducer. An average grain size of 10 microns in the 99.99% aluminum is sufficient to allow enough dislocations to be generated and glide away from the source so that a detectable strain pulse, or acoustic emission pulse, is produced. As the grain size is increased the dislocation glide distance increases and a larger strain pulse is produced. However, as the grain size increases the grain boundary area decreases. This means that there are fewer grain boundary sources of dislocations. Hence a reduction in the emission is to be expected. This happens at a grain size of about 350 microns for the data shown in Fig. 4, and for the threshold level of counting used in theses tests*.

The increase in the amount of acoustic emission that is observed at low frequencies for the large grain sizes can be explained as follows. A large grain size means that the dislocation glide distances are greater than for smaller grain sizes. The dislocations are in motion for a longer time interval and thus more dislocations can be emitted before the source is shut off. From this it can be concluded that the average duration of

*These results will be reported in more detail in the doctoral dissertation of Mr. Robert Bill at the University of Michigan in the latter part of 1970.

the slip events is longer and that the corresponding "effective frequencies" of the acoustic emission (i.e., the reciprocal of the duration of the slip events) are correspondingly lower. As the grain size decreases the source will operate for a shorter time and the "effective frequency" of the acoustic emission increases.

4.0 RESIDUAL STRESS DETERMINATION

The basis on which it is proposed to investigate residual stress in metals by acoustic emission techniques is as follows.

Most metals produce acoustic emission when strained. The amount of emission is related to the stress level, and to the volume of material stressed. For many engineering materials, including steel and aluminum, the emission is found to have the following characteristics:

(1) On repeated loading to a stress below the yield stress of a test specimen the rate of emission is essentially constant and low. The total emission produced on loading to a particular stress level is proportional to the applied stress, as shown in curve "o-a" in Fig. 6.

(2) During the unloading part of the cycle the acoustic emission is negligible for a small decrease in the stress level, then it increases in an exponential manner as shown in curve "a-b" in Fig. 6.

A simplified model that is proposed for a specimen that contains a region of uniform tensile stress and a region of uniform compressive stress, both of the same magnitude, is shown in Fig. 7. Fig. 8 shows the stress levels reached as a result of applying a tensile load "F". Fig. 9 shows the separate cumulative emission from sections A and B of the model in Fig. 7. Fig. 10 is a combined cumulative emission curve.

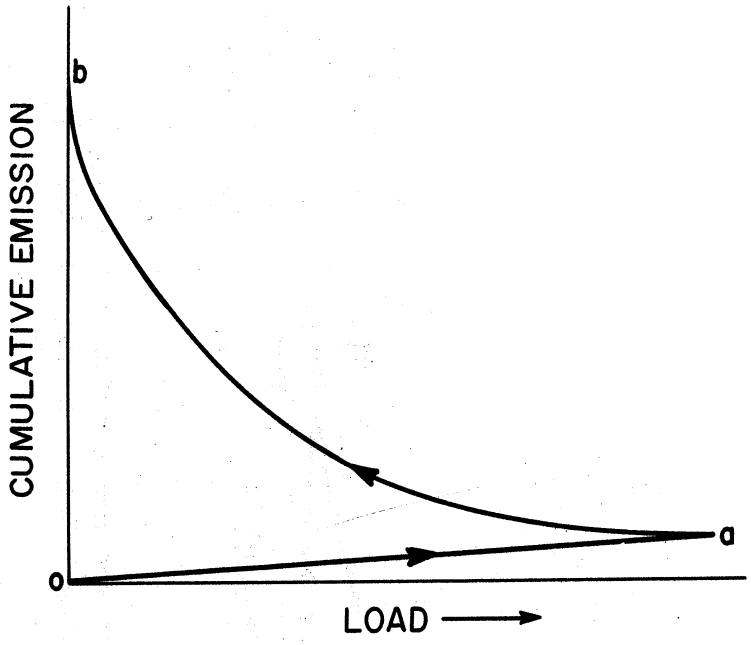

Fig. 6. Repeated loading of a test specimen to stress levels below the yield stress results in the type of cumulative emission versus load curve shown in the figure.

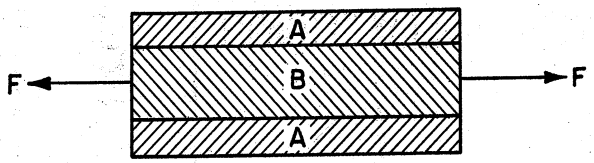

Fig. 7. Simplified model for a specimen containing uniform compressive and tensile stresses. Region A is in tension. Region B is in compression.

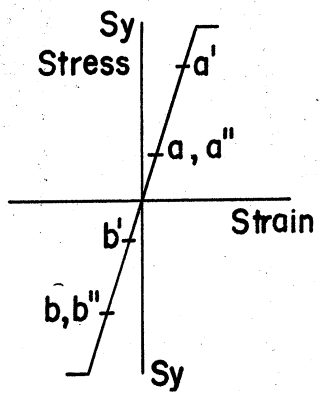

Fig. 8. Stress levels applied to the specimen shown in Fig. 7 in order to obtain the acoustic emission response shown in Fig. 9.

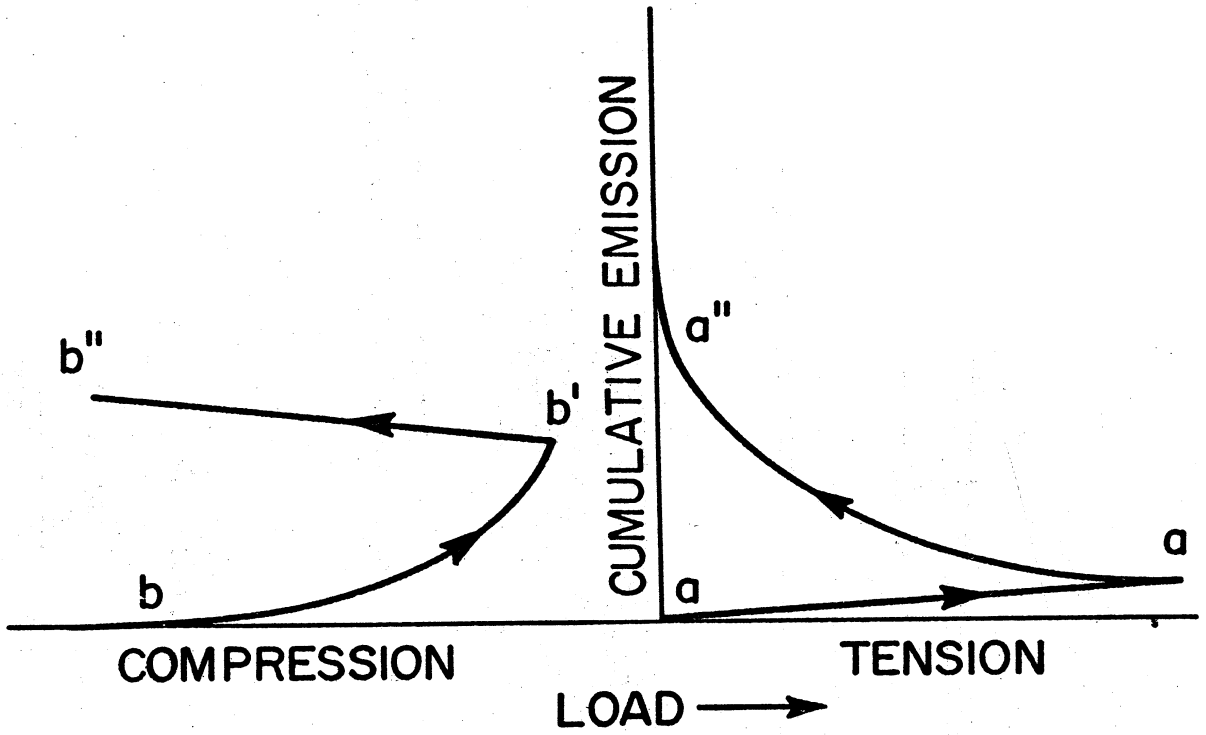

Fig. 9. Schematic diagram of the acoustic emission from the model shown in Fig. 7. Region A emits in the manner shown for the tensile loading. Region B emits in the manner shown for the compressive loading.

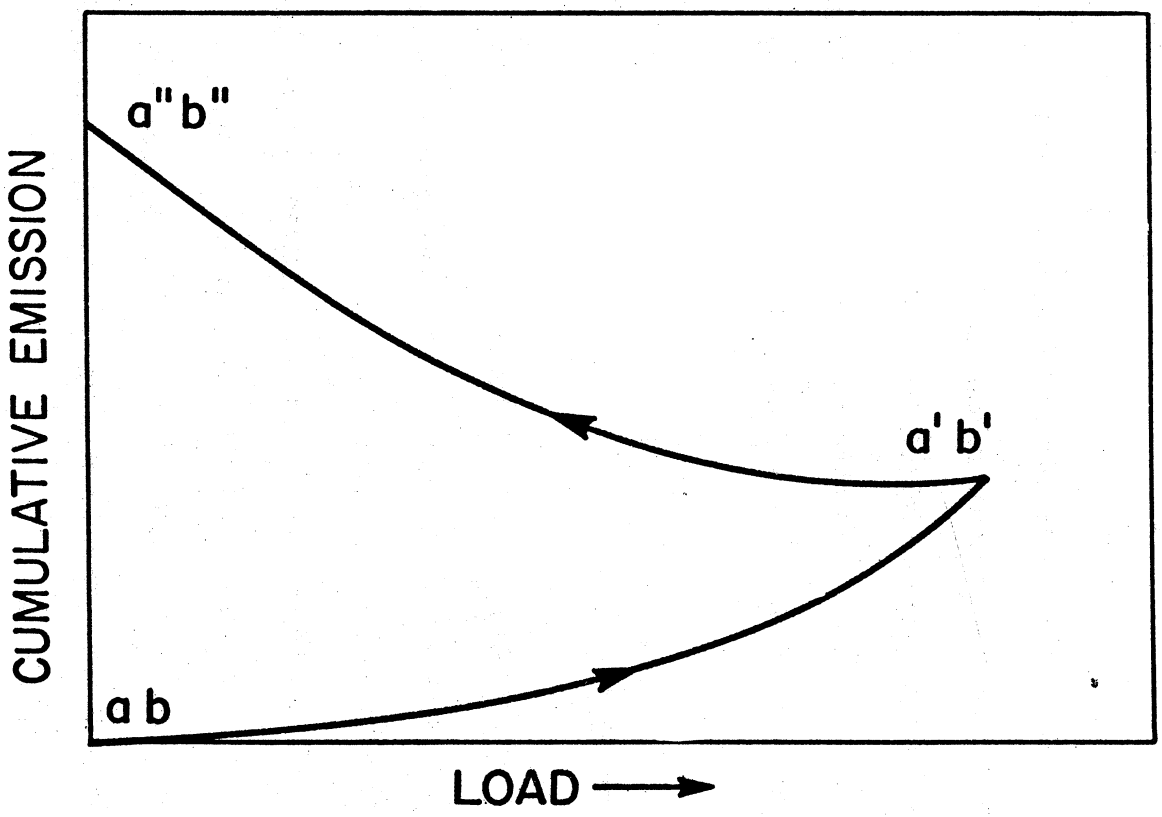

Fig. 10. The combined emission for the model in Fig. 7 is a combination of the two curves shown in Fig. 9.

If a large enough stress is applied to the specimen so that the section that was originally in compression is now subjected to a tensile stress, the cumulative emission curve would appear as shown schematically in Fig. 11.

Hence, in a general case it is necessary to apply a tensile or compressive stress larger than the residual stress and then to observe the shape of the load and the unload cumulative acoustic emission curves. If a curve such as is shown in Fig. 11 is obtained, the change in the slope of the load and unload curves will occur at the peak value of the residual stress.

4.1 EXPERIMENTAL PROCEDURES

Tests have been performed on 1018 steel specimens and on 6061-T6 aluminum. The steel specimens were annealed at 950^{o}F for three hours and the aluminum was tested in the T-6 condition.

The 6061-T6 aluminum specimens were 0.5 in. in diameter 4.0 in. long and had flat surfaces 1.5 in. long and 0.1 in. deep milled on both sides. One of these was tested in the "as-received" condition. Residual stresses were introduced in the other specimen by bending it to an angle of about 1/2 degree and then straightening it.

Three flat specimens of annealed 1018 steel were prepared having a gage section 5/8 in. wide, 1/4 in. thick and 4 in. long. Rectangular slots an inch long and 1/4 in. wide were cut in the center of two of the specimens. A 1018 steel insert 0.0015 in. longer than the slot was shrunk fit into the slot of one specimen. The slot in the other specimen was filled with an insert that was 0.002 in. thicker than the specimen. The specimen was then rolled until the insert was the same thickness as the specimen. The

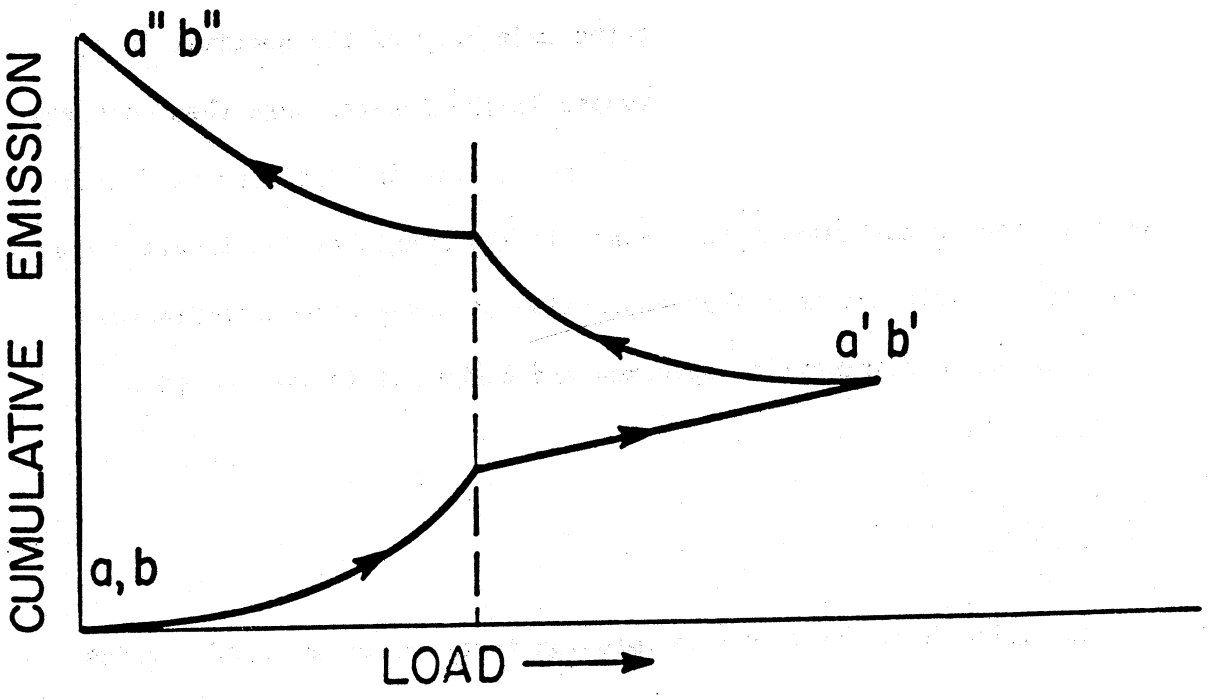

Fig. 11. If a sufficiently large tensile stress is applied to the specimen shown in Fig. 9 so that the region under compression is put into tension, a cumulative emission curve having two points of inflection should result.

compressive stress produced in the insert in this way was reduced subsequently by plastically straining the main body of the specimen in a standard tensile machine. The stresses in the inserts were then measured by the use of strain gages placed on the inserts and applying sufficient tensile load so that no further change in the length of the insert occurred. These tests indicated that the compressive stresses were approximately 16,000 psi in the shrunk-fit specimen and 6,000 psi in the rolled-in specimen.

4.2 RESULTS

The results of the acoustic emission tests on an annealed (stress-free) and the residual stress specimen are shown in Figs. 12-16. The curves shown are reproducible to within $\pm$ 3% on any particular specimen. A pre-load of 50 pounds was maintained on the specimens when making a test, hence the applied load is shown in the Figures as ranging from 50 to 400 pounds. The maximum load of 400 pounds in all tests is less than half the yield stress of the materials.

4.3 DISCUSSION OF RESULTS OF THE RESIDUAL STRESS TESTS

The effect of residual compressive stresses on the acoustic emission from the 6061-T6 aluminum specimen that has been bent about $1/2^{o}$ and restraightened is evident by comparing Figs. 12 and 13. The emission obtained on loading the specimen is greater than when no residual compressive stresses are present and there is an increasing rate of emission on loading up to the stress at which the compressive stress is overcome by the applied tensile stress. This point is indicated by the arrow on

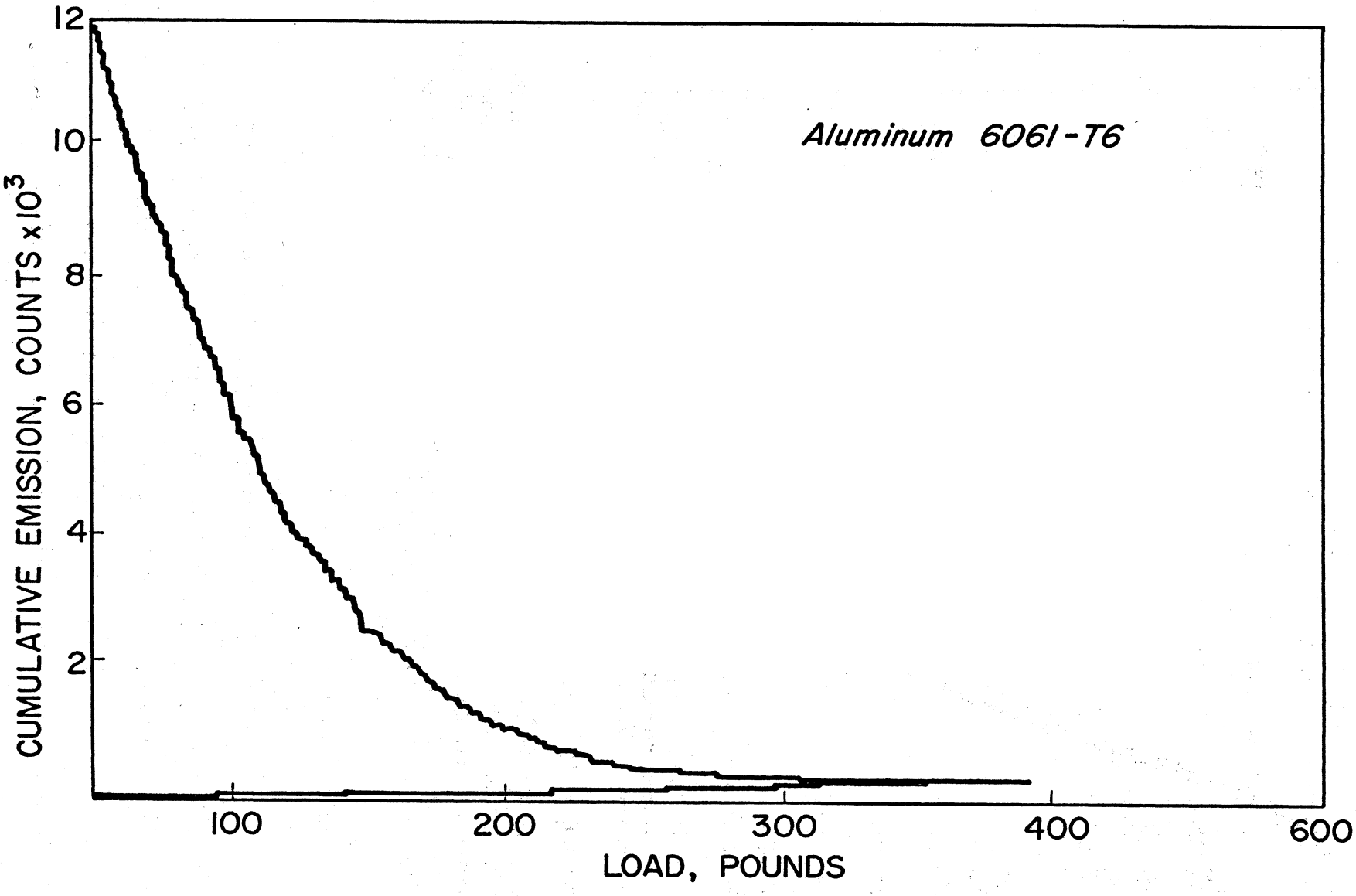

Fig. 12. Cumulative acoustic emission from 6061-T6 aluminum during loading and unloading. The maximum stress applied to the specimen is less than half of the yield stress.

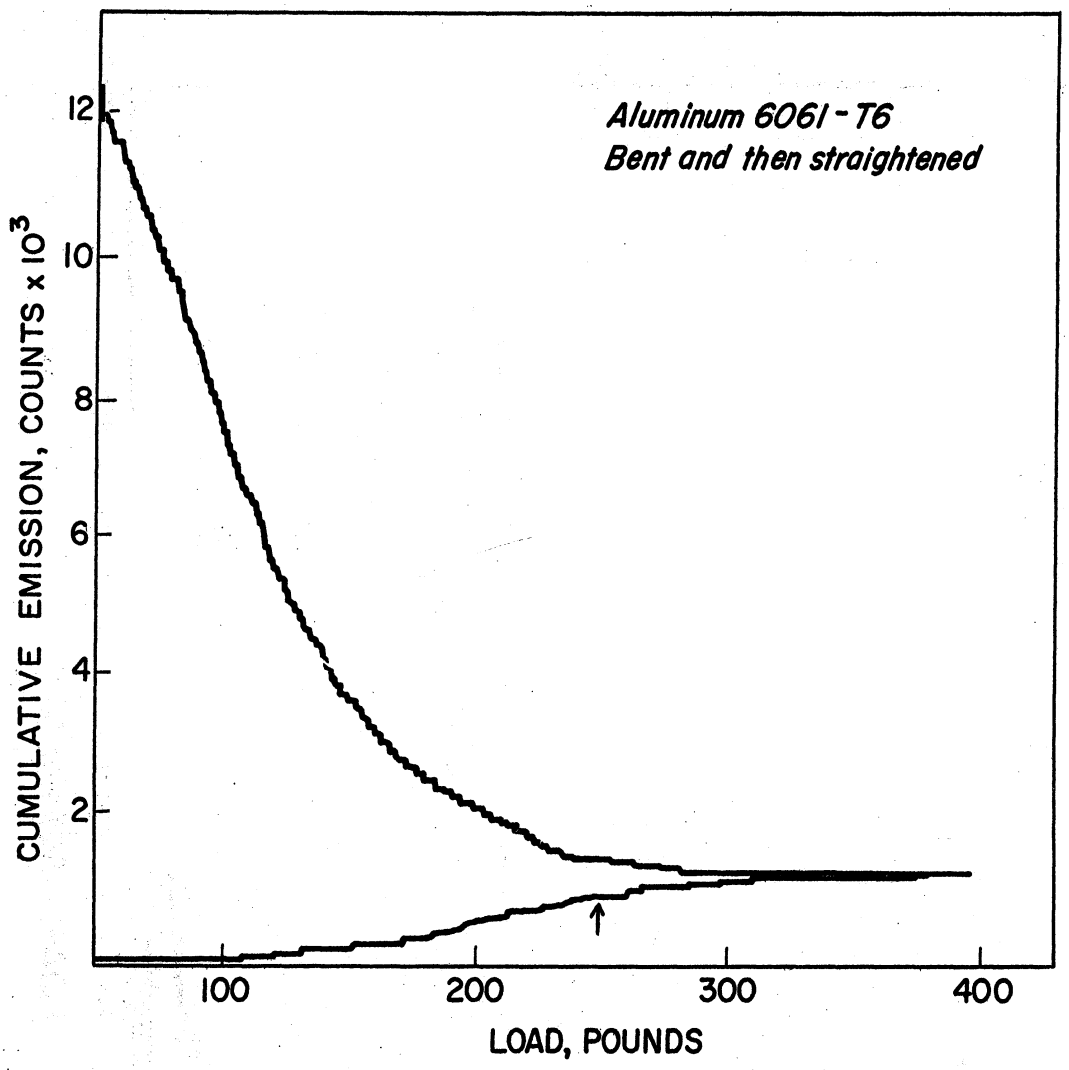

Fig. 13. Cumulative acoustic emission from a 6061-T6 aluminum specimen that had been bent to about 1/2° and then restraightened. The arrow indicates a region of the load curve in which there is a change in slope, as might be expected from the model in Fig. 11. The applied stress is less than half the yield stress.

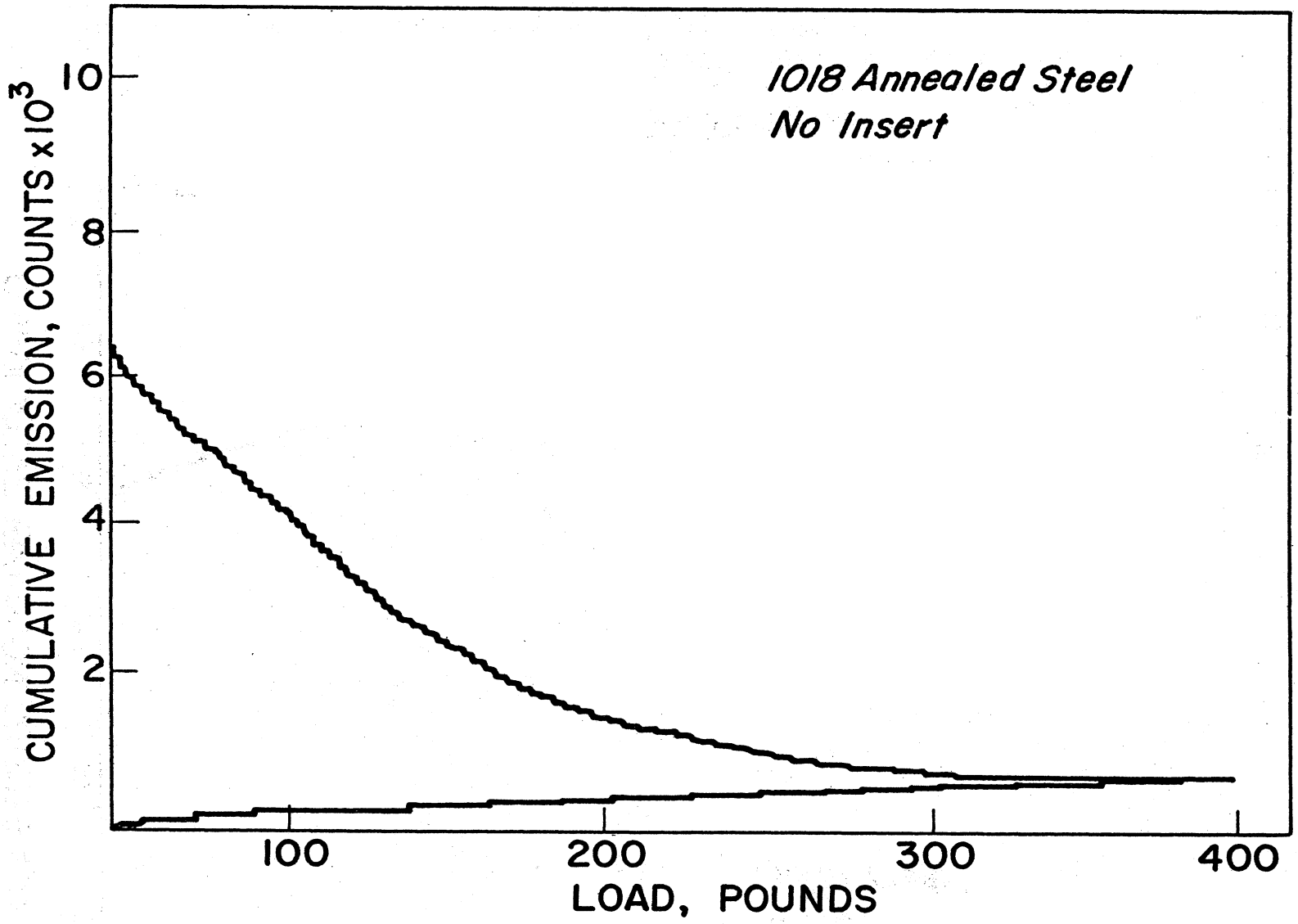

Fig. 14. Acoustic emission from an annealed 1018 steel flat tensile specimen which has no residual stresses.

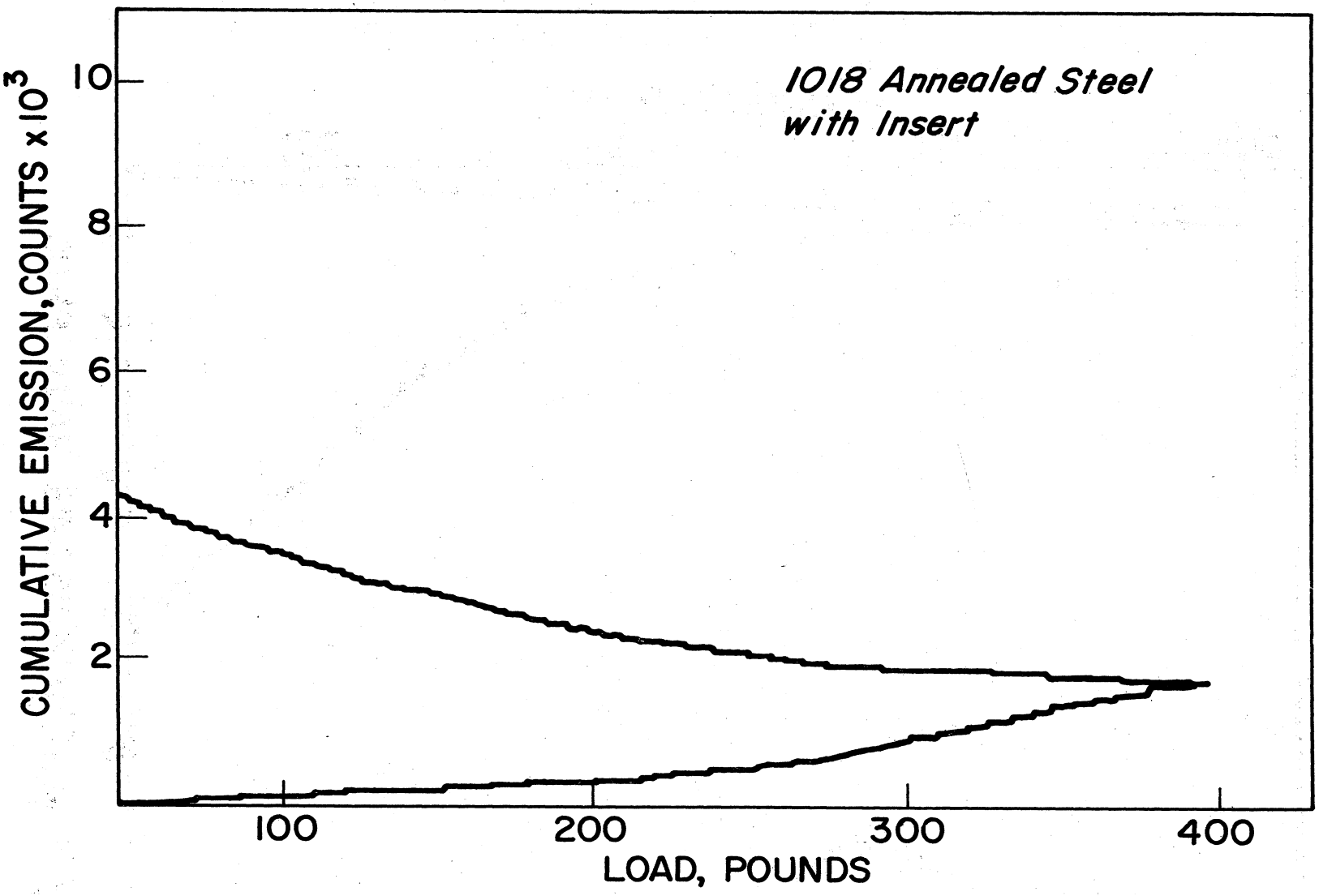

Fig. 15. Acoustic emission from an annealed 1018 steel flat tensile specimen containing a shrunk-fit insert having a compressive stress of about 16,000 psi.

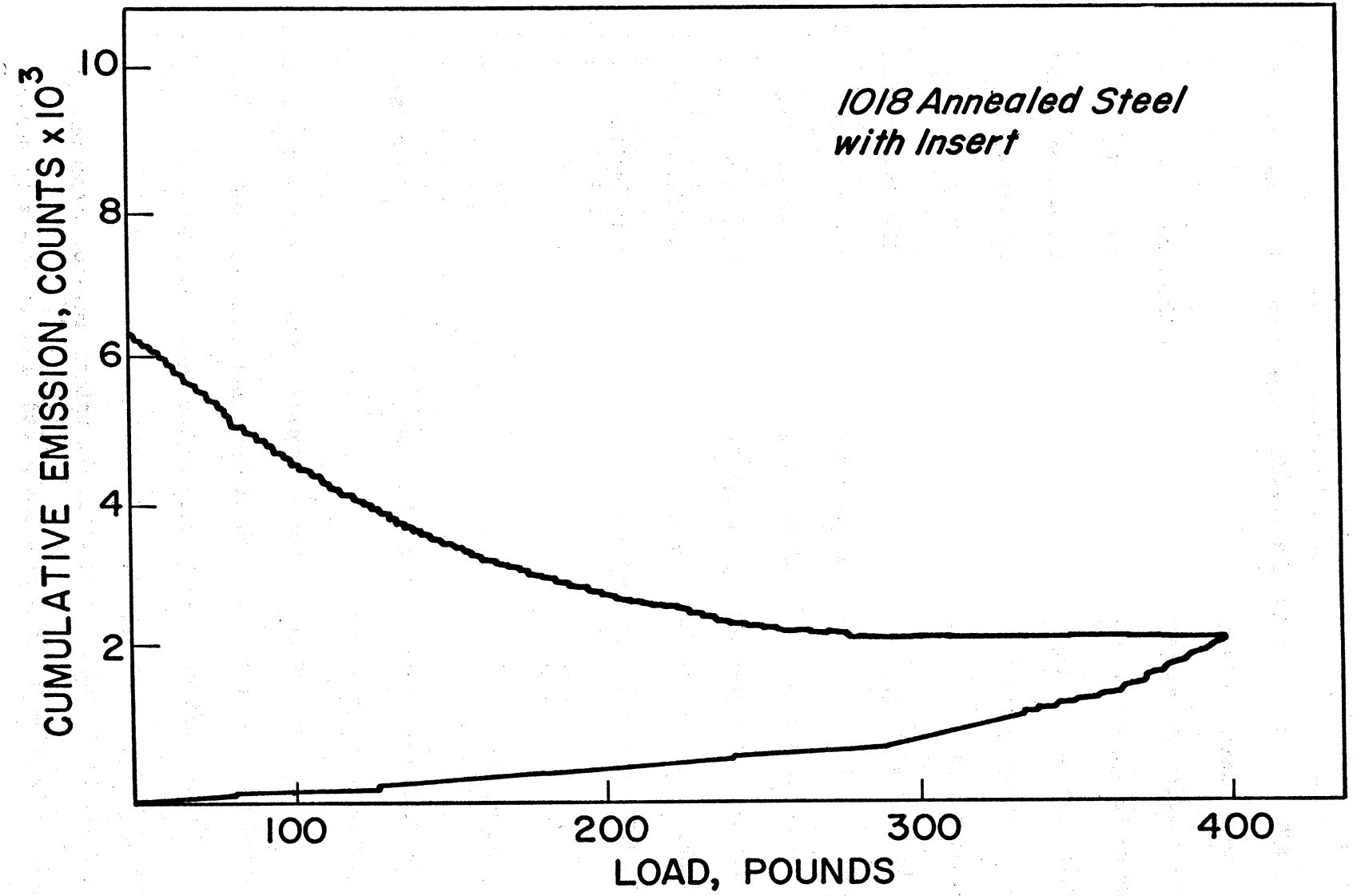

Fig. 16. Acoustic emission froman annealed 1018 steel flat tensile specimen containing a rolled-in insert having a compressive stress of about 6000 psi.

the graph at a load of about 250 pounds. Beyond this load the rate of increase of emission is constant.

According to the model described in Fig. 11 there should be a point of inflection on the unload part of the curve. This is not evident, however, perhaps because of the low value of the unload stress that is associated with that part of the specimen having residual compressive stress.

Fig. 14 shows the emission from a 1018 flat steel specimen having no residual stresses. The constant rate of emission obtained on the application of a load can be noted. In Fig. 15 and 16, however, the emission rate increased during the application of a load. In both specimens it is evident that the applied stress was not sufficient to overcome the residual compressive stress and there is no inflection point on the load curve.

5.0 CONCLUSIONS

The following conclusions can be drawn from the results that have been presented in this report.

(1) The effect of grain size on acoustic emission can be explained by a model based on the activation of dislocation sources and the subsequent shutting off of these sources by the back-stress of dislocation pile-ups.

(2) In those materials in which the unload emission phenomenon is observed it is possible to obtain the unload emission effect by superimposing a tensile stress on a residual compressive stress.

(3) The change in rate of acoustic emission when a residual stress is exceeded by an applied stress of opposite sign may have some promise as a means of determining the magnitude of the residual stress.

6.0 FUTURE EFFORT

No more direct effort will be expended on the effects of microstructure on acoustic emission. It is felt that the work reported here substantiates the model for acoustic emission based on the activation of dislocation sources as proposed by Agarwal, et. al.[1] The model will continue to be applied to the interpretation of the results of acoustic emission tests on the materials tested in future work on the program.

Work is continuing on the determination of residual stress. Efforts will be made to correlate the magnitude of stress as determined by acoustic emission with the results of destructive measurements of stress.

An investigation of creep and fatigue phenomena is continuing, along with low noise level loading techniques.

REFERENCES

1. Agarwal, A.B.L., Frederick, J.R. and Felbeck, D.K., "Detection of Plastic Microstrain in Aluminum by Acoustic Emission", Metallurgical Transactions, Vol. 1, p. 1070, April 1970

2. Sankar, N.G., "Unload Emission Behavior of Materials and Its Relation to the Bauschinger Effect", Ph.D. Thesis, University of Michigan, Ann Arbor, Michigan, 1969.

REPORT DISTRIBUTION LIST

1. Mr. John F. Moore
   North American Rockwell Corp.
   Los Angeles Division
   International Airport
   Los Angeles, California 90009

2. Dr. J. R. Frederick
   University of Michigan
   Dept. of Mechanical Engineering
   2046 East Engineering
   Ann Arbor, Michigan 48105

3. Mr. Allen T. Green
   Aerojet-General Corp.
   Materials Integrity Group
   Dept. 0729, Bldg. 2931
   Sacramento, California 95813

4. Professor R. H. Chambers
   Dept. of Physics
   Engineering Experiment Station
   University of Arizona
   Tucson, Arizona 85721

5. Professor Stuart A. Hoenig
   Dept. of Electrical Engineering
   Engineering Experiment Station
   Univ. of Arizona
   Tucson, Arizona 85721

6. Mr. Eugene Roffman
   Frankford Arsenal
   Fire Control Laboratories
   Philadelphia, Pa. 19137

7. Mr. Solomon Goldspiel
   U.S. Naval Applied Science Laboratory
   Flushing and Washington Avenues
   Brooklyn, N. Y. 11251

8. Mr. Otto Gericke
   Test and Evaluation Methods
   Army Material Command
   Army Materials & Mechanics Research Center
   Watertown, Massachusetts 02172

9. Mr. D. D. Skinner
   Fellow Engineer
   Westinghouse Electric Corp.
   Research Laboratories
   Pittsburgh, Pa. 15235

10. Lt. Col. Louis Klinker, U.S. Army
    Office Chief of Research & Development
    Materials Sciece & Technology Branch
    Highland Building
    3045 Columbia Pike
    Arlington, Virginia 22204

11. Mr. Edward Criscuolo
    Naval Ordinance Laboratory
    Radiation Physics Division (code 223)
    White Oak
    Silver Spring, Maryland 20910

12. Mr. Stephen D. Hart
    Naval Research Laboratory
    Mechanics Division
    Washington, D.C. 20390

13. Dr. A. S. Tetelman, Head
    Materials Division
    College of Engineering
    Univ. of California
    Los Angeles, Calif. 90024

14. Dr. L. W. Orr
    Dept. of Electrical Engineering
    Univ. of Michigan
    Ann Arbor, Michigan 48105

15. Professor Emmett N. Leith
    Dept. of Electrical Engineering
    Univ. of Michigan
    Ann Arbor, Michigan 48105

16. Mr. F. S. Williams
    Aero Materials Dept.
    Naval Air Development Center
    Warminster, Pa. 18974

17. Mr. J. L. Kreuzer
    Optical Group
    Perkin-Elmer
    Norwalk, Connecticut 06850

18. Professor R. C. McMasters
    Nondestructive Testing Research Lab
    Dept. of Welding Engineering
    The Ohio State University
    Columbus, Ohio 43210

19. Dr. Volker Weiss
Assoc. Chairman
Dept. of Chemical Engineering
& Metallurgy
Syracuse University
Syracuse, New York 13210

20. Professor Lawrence Mann, Jr.
Dept. of Mechanical, Aerospace, &
Industrial Engineering
Louisiana State Univ.
Baton Rouge, Louisiana 70803

21. Howard A. Johnson
The Boeing Company
Space Division, Aerospace Group
Kent Facility
P.O. Box 3868
Seattle, Washington 98124

22. C. Gerald Gardner
Southwest Research Institute
8500 Culebra Road
San Antonio, Texas 78206

23. Mr. Carlton H. Hastings
Chief, NDT Evaluation
AVCO Corp., Space Systems Div.
Lowell Industrial Park
Lowell, Mass. 01851

24. Mr. David Driscoll
U.S. Army Materials & Mechanics
Research Center
Watertown, Mass. 02172

25. Dr. R. L. Gause
Materials Division
Marshall Space Flight Center
Huntsville, Alabama 35800

26. 3 copies to:
AFML/MAMN
Attn: Lt. James W. Bohlen
APAFB, Ohio 45433

27. 20 copies to:
Defense Documentation Center DDC
Cameron Station
Alexandria, Virginia 22314

28. 3 copies to:
Director of Advanced Research
Projects Agency
Washington, D.C. 20301

29. The Institute for Defense Analysis
400 Army-Navy Drive
Arlington, Virginia 22202

30. The Nondestructive Testing
Information Service
Watertown Arsenal
Watertown, Mass. 02172

31. Pravin G. Bhuta, Manager
Applied Mechanics Laboratory
Systems Group of TRW Inc.
One Space Park
Redondo Beach, Calif. 90278

32. T. Theodore Anderson
Argonne National Laboratory
Reactor Engineering Division
D308
9700 S. Cass Avenue
Argonne, Ill. 60439

33. Phil Hutton & D. C. Worlton
Battelle-Northwest
P.O. Box 999
Richland, Washington 99352

34. Robert Moss
Boeing Scientific Research Lab.
1-8000
MS 01-14
Box 3981
Seattle, Washington 98124

35. Charles Musser
The Boeing Company
Saturn Booster Branch
Org. 5-1752
MS LE-62
Box 29100
New Orleans, La. 70129

36. Harvey L. Balderston
The Boeing Company
Space Division, Kent Facility
P.O. Box 3868
Seattle, Washington 98124
Attn: Orgn. 2-5022
Mail Stop 84-38

37. Thomas F. Drouillard
Dow Chemical Co.
Rocky Flats Division
P.O. Box 888
Golden, Colorado 80401

38. R. E. Ringsmuth
Jet Propulsion Laboratory
California Institute of
Technology
4800 Oak Grove Drive
Pasadena, Calif. 91103

39. Dwight Parry
Phillips Petroleum
P.O. Box 2067
Idaho Falls, Idaho 83401

40. Brad Schofield
Teledyne Materials Research
303 Bear Hill Road
Waltham, Mass. 02154

41. Hal Dunegan
University of California
Lawrence Radiation Laboratory
P.O. Box 808
Livermore, Calif. 94550

42. C. D. Bailey
Lockheed-Georgia Co.
Materials Development Laboratory
Dept. 72-14
Marietta, Georgia 30060

43. R. F. Saxe
North Carolina State Univ.
Nuclear Engineering Dept.
P.O. Box 5636
Raleigh, N. C. 27607

44. John G. Sessler
Materials Science
Syracuse University Research Corp.
Merrill Lane
Syracuse, N.Y. 13210

45. L. J. Chockie
General Electric Company
175 Curtner Avenue
San Jose, Calif. 95125

46. Lawrence Radiation Laboratory
Attn: Technical Information Dept L-3
P.O. Box 808
Livermore, Calif. 94550

47. James Bryant
Office Chief of Res. & Development
Attn: CROPES
3045 Columbia Pike
Arlington, Va. 22204

48. H. E. Pearce
McDonnell Douglas Corporation
1100 17th Street, N.W.
Washington, D.C. 20036

49. Jay M. Stevens
Naval Air Systems Command
Code AIR-52055
Washington, D.C. 20360

50. Mr. Steve Ezangelities
Dept. 263, Mail Station 8
McDonnell Douglas, Western Division
3000 Ocean Park
Santa Monica, Calif. 90406

51. Dr. Harold Berger
Group Leader, Nondestructive Testing
Metallurgy Division
Argonne National Laboratory
9700 South Cass Avenue
Argonne, Ill. 60439

52. Dr. Karl Graff
The Ohio State University
Engineering Mechanics Department
212 Boyd Laboratory
155 W. Woodruff Avenue
Columbus, Ohio 43212

53. Mr. J. C. Spanner
NDT Consultant, FFTF Project
Battelle Memorial Institute
Pacific Northwest Laboratories
P.O. Box 999
Richland, Washington 99352

54. Dr. George Martin
Branch Chief
Advanced Fabrication Development Dept.
A253, Mail Station 5
McDonnell Douglas Astronautics
Santa Monica, California 90506